Colloid Polym Sci 277:1186–1192 (1999)

ORIGINAL CONTRIBUTION

B. Trahasch
H. Frey
K. Lorenz
B. Stühn

Dielectric relaxation in carbosilane dendrimers with cyanobiphenyl end groups

Received: 9 June 1999
Accepted in revised form: 21 July 1999

B. Trahasch
Fakultät für Physik
Albert-Ludwigs-Universität
Hermann-Herder-Strasse 3
D-79104 Freiburg, Germany

B. Stühn (✉)
Technische Physik II/Polymerphysik
TU-Ilmenau, Postfach 100565
D-98684 Ilmenau, Germany
e-mail: bernd.stuehn@physik.tu-ilmenau.de
Tel.: +49-3677-693671
Fax: +49-3677-693770

H. Frey · K. Lorenz
Institut für Makromolekulare Chemie und
Freiburger Materialforschungszentrum
Stefan-Meier-Strasse 21/31
D-79104 Freiburg, Germany

Abstract Carbosilane dendrimers of generation 1 and 2 are functionalized with mesogenic end groups (cyanobiphenyl) via spacers of 5 and 11 carbons. The dielectric relaxation is measured over broad frequency (1 Hz–1 GHz) and temperature (170–470 K) ranges. Two relaxation regimes are observed and characterized as δ and β relaxation. The δ relaxation is nearly a single Debye process and varies strongly with temperature. The S_E to S_A transition observed for the dendrimers with long spacers causes a jump in the relaxation rate of the δ process. The β process displays an Arrhenius-type temperature dependence with an activation energy of 35 kJ/mol. The relaxation time depends on spacer length. The dielectric relaxation reflects the mutual distortion of the dendrimer scaffold and the smectic layers.

Key words Dendrimers · Dielectric spectroscopy

Introduction

The combination of mesogens with amorphous polymer chains has led to an exciting new class of materials [1]. In many cases they unite the desired properties of an optically anisotropic stable glass with the ease of processing due to low melt viscosity. The thermodynamic characteristics of a liquid-crystalline polymer (LCP) are summarized by its glass-transition temperature, T_g, and the transition temperatures between liquid-crystalline phases. These are in turn the result of the segmental mobility of the macromolecule and the opposition between its amorphous structure and the drive of the mesogens to attain an ordered state. In order to tailor the properties of LCPs various routes have been followed. Traditionally, connecting mesogenic units to a polymer may be done by attaching them as side groups leading to side-chain LCPs or alternatively incorporating them into the polymer chain as a main-chain LCP.

A key point that defines the liquid-crystalline properties of side-chain LCPs has turned out to be the length of a flexible spacer between the mesogen and the polymer chain. It is found that decoupling of the mesogen from the polymer chain by increasing the spacer length tends to lower T_g and to enhance the liquid-crystalline order.

A new approach in the design of LCPs is introduced by using branched polymer structures. The primary effect is to hamper crystallization [2]. This concept has recently been extended to the case of hyperbranched macromolecules and perfect dendrimers. Their end groups may be functionalized with mesogenic groups. Flexible spacers are inserted between the macromolecule and the mesogen. Due to their perfect structure den-

drimers are particularly well suited for a systematic study of the influence of branching on the segmental dynamics and the liquid-crystalline order.

In the present paper we report the results of the dielectric spectroscopy of carbosilane dendrimers with mesogenic end groups. The mesogen employed in this study is a cyanobiphenyl and it is attached to the dendrimer via alkyl spacers of different length. The synthesis and the thermal properties of these materials have been described in a previous publication [3].

The same dendritic core has previously been functionalized with rodlike molecular units ($-C_6F_{13}$) resulting in materials with a domain structure that depended strongly on the generation of the dendrimer [4]. The generation 1 dendrimer exhibited a lamellar structure thus enabling the perfluorinated end groups to arrange in their preferred type of layered order. With increasing generation the spherical architecture of the dendrimer core plays an increasingly important role and the lamellar structure is replaced by more complex structures with curved end group layers. The segmental dynamics in these macromolecules has been studied using quasielastic neutron scattering (QENS) [5] as well as dielectric spectroscopy [6]. The scattering experiment offers the possibility to investigate the molecular dynamics in both space and time. Moreover, due to the chemical structure of the dendrimers used, they were intrinsically labeled for the scattering of neutrons. The scattering from the dendrimer core was dominated by the incoherent scattering from hydrogen, whereas the end groups scattered coherently. It was thus possible to separate the dynamics from the core and the shell of the dendrimer. As a result the segmental dynamics of the dendrimer core was characterized as a jump-diffusion process. The effect of the end groups on the internal dynamics was seen as a strong decrease in the segmental diffusion coefficient. This was concluded from a comparison of a nonfunctionalized dendrimer with the functionalized analogue. An increase in generation further decreases the segmental diffusion coefficient. The dynamics of the end groups on the other hand was found to be a rotational diffusion around their long axis. The rotational diffusion coefficient varied only weakly with generation in accordance with the observation that the local order between end groups remains nearly the same for generations 2 and 3.

The time resolution of the neutron spectrometer used is limited to energy transfers in the range of micro-electron volts corresponding to relaxation times of the order of 10^{-10} s. Dielectric spectroscopy complements this dynamic regime with its wide range of accessible frequencies from 1 to 10^8 Hz. The method does not offer spatial resolution, however, and cooperative effects in the dynamics are measured in an integral manner. For the same dendrimers a strong relaxation was observed consisting of two components with a temperature dependence described by the Vogel–Fulcher law in accordance with the observed T_g. The microscopic origin of the relaxation was seen in the fluctuation of a dipole moment parallel to the long axis of the end group. It is therefore to be compared to the δ process found in side-chain LCPs [7]. A fast relaxation with weak Arrhenius-type temperature dependence was observed with a significantly smaller relaxation strength. It was still slower than the rotational diffusion of the single end group as determined with QENS but was tentatively assigned to this same molecular origin.

The aim of this investigation is to use a well-studied mesogenic unit attached to the same dendritic scaffold used in previous studies. The strong dipole moment of the mesogen makes it particularly suitable for dielectric spectroscopy. The experimental results cover a wide range of frequency and temperature. We present results from measurements of three different dendrimers: two samples of generation 1 with different spacer length between dendrimer and end group and one dendrimer of generation 2 with the same long spacer.

Experimental

The dielectric measurements were performed with two different experimental set-ups in order to cover a wide frequency range:

1. Measurements in the frequency range from 2 Hz to 300 kHz were carried out using a Schlumberger 1260 impedance analyser. Details of this set-up were given previously [8].

2. For high frequencies in the range between 1 and 1000 MHz we used a Hewlett-Packard HP-4191-A impedance analyser, which is based on the principle of a reflectometer.

Measuring the reflectivity of a capacitor for an electromagnetic wave enables the determination of the complex impedance of the sample. The capacitor used consists of two gold-covered plates, separated by a 50-μm glass-fiber spacer (to define an exact sample thickness). The capacitor filled with the sample was assembled as a part of the wave guide of the reflectometer. This arrangement was placed in a cryostat. By use of a temperature-controlled nitrogen gas jet, temperature variation between 170 and 470 K is possible. Temperature stability was better than 0.5 K. The sample temperature was measured directly at the capacitor using a platinum resistor.

The filled capacitor was annealed at 100 °C under light pressure to adjust the distance of the plates to the value defined by the spacer material. Ten frequencies were measured within each decade and the error was estimated by repeating each measurement 3 times, and for the high-frequency range 10 times. The temperature variation was in steps of 3–5 °C and the sample was allowed to equilibrate after each change of temperature. Heating and cooling cycles were compared and the results reported here refer to the cooling run. No differences were found between heating and cooling above T_i (Table 1). The S_A phase was supercooled in the cooling runs.

Details of the synthesis of the samples were given previously [3]. Mesogen-substituted carbosilane dendrimers bearing 12 and 36 cyanobiphenyl groups accordingly are designated Gx-My, with x representing the generation number (1 or 2). The subscript y is equal to 5 or 11, reflecting the number of carbons of the spacer between the dendrimer and the mesogens.

The DLCPs (dendritic LCP) based on dendrimer generation G1 and generation G2 were obtained via a reaction between 5-((4′-

Table 1 Thermal properties of the dendrimers

	T_g(°C)	$T_{S_E \rightarrow S_A}$ (°C)	T_i (°C)	$\Delta H_{S_E \rightarrow S_A}$ (J/g)	ΔH_i (J/g)	ΔS_i [J/(K mol end groups)]
G1-M5	17	–	98	–	3.0	2.9
G1-M11	14	67	106	32	8.8	10.4
G2-M11	7	61	130	31	8.2	9.2

cyano(1,1′-biphenyl)-4-yl)oxy)valeric acid or 11-((4′-cyano(1,1′-biphenyl)-4-yl)oxy) un-decanoic acid (G*x*-M5 and G*x*-M11, respectively; see Scheme) and dendritic polyols based on carbosilane scaffolds [5]. Successful and easy access to fully mesogen substituted dendrimers was achieved by application of diisopropylcarbodiimide as an acid-activating agent, using the 4-(dimethylamino)pyridinium salt of *p*-toluenesulfonic acid as a catalyst. Details of the synthesis are described elsewhere [3].

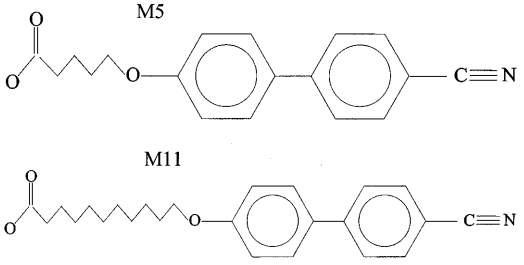

Results and discussion

The thermal and structural properties of G1M5, G1M11 and G2M11 have been discussed in a previous publication [3]. Here we only report the main results that are of importance for the interpretation of the dielectric relaxation behavior. We first summarize the thermal properties as determined by differential scanning calorimetry (DSC) measurements and briefly discuss the domain structure and the mesogenic order as revealed by X-ray scattering experiments. We then proceed to the results of the dielectric spectroscopy measurement.

The DSC heating curves for G1M5, G1M11 and G2M11 are shown in Fig. 1. The transition temperatures and enthalpies are compiled in Table 1. A clear difference is observed between the generations 1 and 2 dendrimers. There is only one endothermic peak in the G1M5 diagram. It defines the transition from a liquid-crystalline to an isotropic phase as confirmed by the textures observed between crossed polarizers. The mesophase is of the smectic A (S_A) type. Both dendrimers with long spacers (G*x*M11) exhibit two endothermic peaks. The transition at lower temperature occurs at roughly the same temperature for both dendrimers. The properties change from a highly viscous state to a fluid, birefringent phase at elevated temperature. The second peak then marks the transition to the isotropic phase and is therefore the equivalent of the peak seen for G1M5. The transition enthalpy is larger for the low-temperature transition. On reducing its value

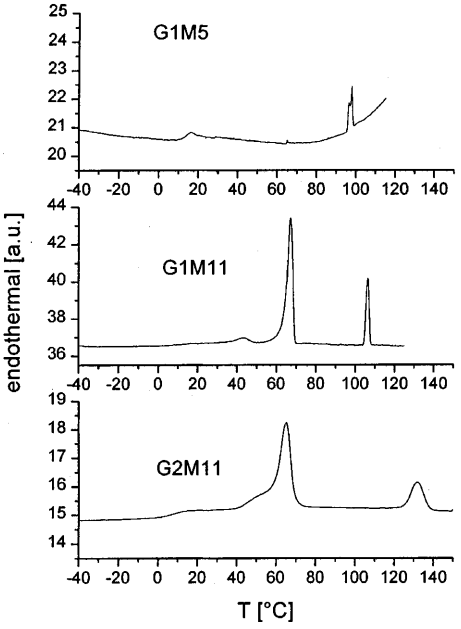

Fig. 1 Differential scanning calorimetry traces during heating: heating rate 20 °C/min. All dendrimers show a glass transition and a transition from smectic to isotropic. Only the dendrimers with long spacers have an additional low-temperature transition

Table 2 Line-shape parameters for $\varepsilon''(\nu)$ for the δ relaxation

	G1-M5	G1-M11	G2-M11
α	0.94–0.98	0.63–0.99	0.71–0.99
γ	≈1.0	≈1.0	0.77–1

to the transition entropy per end group (Table 2) one finds a significantly larger value for G2M11 compared to G1M5. This points to a higher degree of order in the mesophase of G*x*M11 dendrimers. The transition to the low-temperature phase is apparently accompanied by metastable states: annealing the sample at room temperature gives rise to the shoulder in the DSC diagram of G2M11 below the low-temperature transition. A T_g is observed for all samples (Table 1): it decreases with spacer length and with generation thus indicating an increase in segmental mobility.

The S_A-type structure of the mesophase found for G1M5 is confirmed by X-ray scattering experiments. The period of the smectic structure is found to depend only on the length of the mesogen and the spacer length

and not on the dendrimer generation. The average distance between the cyanobiphenyl units is estimated from the wide-angle scattering to be 4.0 Å. In the case of both G1M11 and G2M11 this distance is 4.6 Å. More detailed analysis of the wide-angle reflection reveals a slightly closer lateral packing of the mesogens in G2M11. The difference in the mesogen distance is 1%. The spacer length alone defines the distance of the mesogenic units. Below the lower transition temperature the dendrimers with spacer length 11 develop the lateral order of the mesogens within the smectic layers. This is again revealed by X-ray scattering, which shows additional reflections in the wide-angle regime. These are indexed on the basis of a two-dimensional orthorhombic packing of the mesogens. This type of order has previously been found in LCPs [10] and its denoted as smectic E (S_E). Our data do not allow us to discriminate between parallel and tilted alignments of the mesogens with respect to the layer normal.

The temperature variation of the dielectric spectroscopy data is expected to reflect the glass transition of the material as well as changes in order at the phase transitions. The strongest dipole moment that is present in the dendrimers is that of the mesogenic end group. Its longitudinal component comes from the CN group and is about 4.2 D [11]. An additional transverse component of 1–2 D is expected from the oxy group. The mesogen is connected to the dendrimer scaffold via a -COO- group (see Scheme) which also carries a dipole moment. The spectrum of the three dendrimers in this series exhibits two relaxation regimes that differ in their relaxation strength as well as in their temperature dependence. As an example the dependence of the loss part of the dielectric function ε'' on frequency, ν, and temperature is shown for G2M11 in Fig. 2.

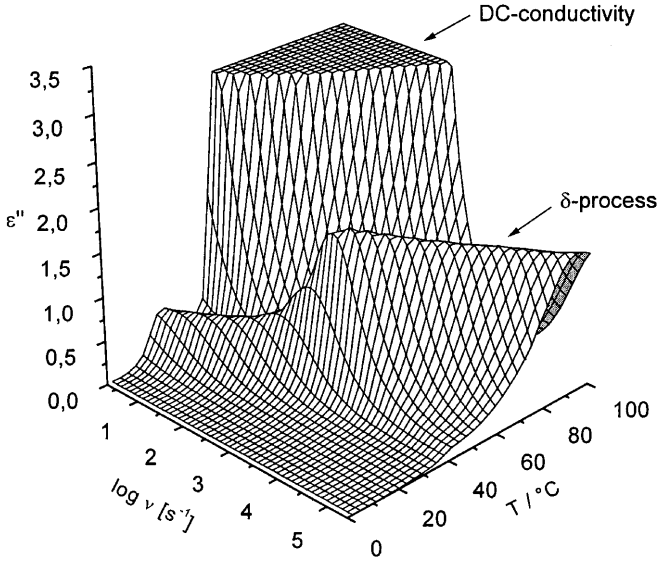

Fig. 2 Dependence of dielectric loss on temperature and frequency for G2M11. The scale of ε'' is cut in order to show the δ process more clearly. Direct current (d.c.) conductivity dominates at low frequency

The low-frequency regime shown in Fig. 2 is dominated by one strong relaxation, which is characterized by a strong temperature dependence. At very low frequencies the dielectric loss shows a direct current (d.c.) conductivity contribution. Above 100 °C this loss component is dominant and only data up to this temperature are presented. With a decrease in temperature a second process moves into the frequency window of the spectrometer. The maximum ε'' is 10 times smaller than the value of the high-temperature process. The position of the maximum ε'' varies only weakly with temperature; however, this shift is sufficient to push it out of the spectral range of the spectrometer at high temperatures. We can follow its temperature variation to higher frequency with the help of the reflectometer. The data show a relatively large scatter as a consequence of the limited resolution at low losses. Following the naming convention in the literature for LCPs we call the strong relaxation a δ process, whereas the high-frequency relaxation is referred to as a β process [7].

The detailed functional form of $\varepsilon''(\nu)$ is well described by a Havriliak–Negami (HN) function [12]

$$\varepsilon^*(\nu) = \varepsilon_\infty + \frac{\Delta\varepsilon}{[1 + (i2\pi\nu\tau)^\alpha]^\gamma} \quad , \tag{1}$$

where $\Delta\varepsilon = \varepsilon_{st} - \varepsilon_\infty$ is the relaxation strength, and ε_{st} and ε_∞ are the permittivities at low and high frequency, respectively. The parameter α characterizes a symmetrical broadening and the parameter γ an asymmetrical broadening of $\varepsilon''(\nu)$ if plotted on a logarithmic ν axis ($0 < \alpha,\ \gamma \leq 1$). In the case of $\alpha = 1 = \gamma$ the HN function reduces to a Debye relaxation process. Special cases are the Cole–Cole function ($\alpha < 1,\ \gamma = 1$) or the Cole–Davidson function ($\alpha = 1,\ \gamma < 1$).

For the δ relaxation we find a good description of the data provided by a HN-type function. This is demonstrated in Fig. 3.

$\varepsilon''(\nu)$ is fitted using the sum of Eq. (1) and a term $\sigma_0/\varepsilon_0(2\pi\nu)$, thus taking into account the d.c. conductivity, σ_0. Both components are shown in the fit as separate curves. In all cases γ is close to 1 and the Cole–Cole-type function is found to be a good fit to the data. G1M5 shows particularly small broadening and its δ process is nearly a single Debye relaxation. Details of the lineshape parameters obtained from the fits are given in Table 1. α decreases with decreasing temperature, indicating a broadening of the relaxation-time distribution. Although our measurements were performed on unoriented samples the width of the δ process is very small even compared to oriented LCPs [3]. A contribution from the segmental dynamics of the dendrimer, which would be called an α process may therefore be excluded. No splitting is observed for the δ process as opposed to the low-frequency process found for the same type of

dendrimers with -C_6F_{13} end groups. In a measurement of an unoriented sample in a S_A phase the dielectric relaxation comprises both the correlation of the dipole moment parallel and perpendicular to the main axis. The nematic potential is expected to separate both on the frequency scale [14]. The observed single relaxation is in accordance with the assumption of only a parallel component of the dipole moment in the mesogen [15].

A similar analysis may be carried out for the β process. Although the experimental resolution is limited in the high-frequency regime the line shape of $\varepsilon''(\nu)$ may be characterized in the full temperature range. An example is given in Fig. 4 for sample G2M11.

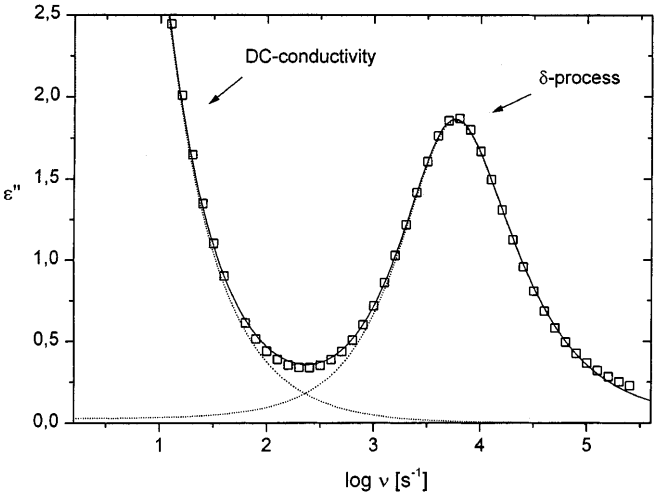

Fig. 3 Example for the analysis of the loss curves using the Havriliak–Negami (*HN*) equation. Data are for G2M11 at 326 K. The *solid curve* is the fit, *dotted lines* represent the components of the d.c. conductivity and the δ process

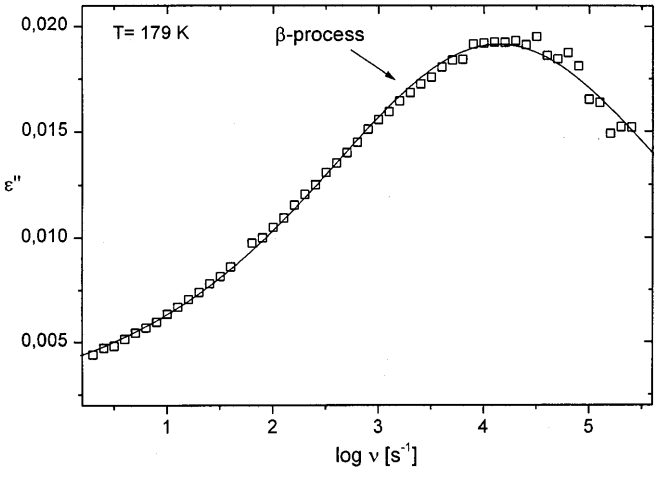

Fig. 4 Loss curve for G2M11 at 179 K. The β process is seen as a broad relaxation which is well described with the HN equation. (*solid curve*)

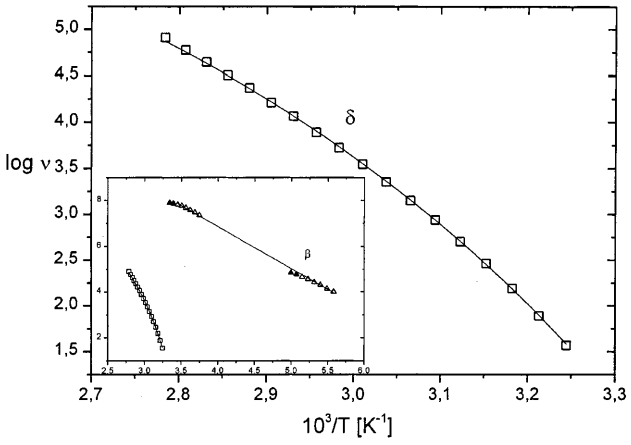

Fig. 5 Overview of the temperature dependence of the β and δ processes for G1M5. The temperature dependence of the δ process is described by a Vogel–Fulcher expression (*solid line*). The *inset* includes the β process. Both experimentally accessible frequency are regimes are described by the same line corresponding to an Arrhenius-type temperature dependence

The relaxation regime is very broad and a fit using the HN equation is restricted to the case $\gamma = 1$. The relaxation is then described by a symmetrical broadening with $\alpha \approx 0.5$ at low temperature and slightly smaller values ($\alpha \approx 0.35$–0.4) at high temperature. The relaxation strength of the β process is in the range 0.12–0.15 for GxM11 and is 0.22 for G1M5.

Turning to the temperature dependence of the dielectric spectra we find a continuous variation for G1M5, whereas the phase transition S_E–S_A for GxM11 is seen as a discontinuity in the temperature dependence. In Fig. 5 we display the values of τ^{-1} as determined from the fit of the HN equation for G1M5. The δ relaxation clearly shows a nonlinear dependence on reciprocal temperature. It is phenomenologically described by the Vogel–Fulcher law:

$$\ln \tau^{-1} = A - \frac{B}{T - T_v} \quad . \tag{2}$$

The limiting temperature, T_v, was kept fixed at $T_v = T_g - 50$ K in the fit shown in Fig. 5 in order to avoid ambiguity in the determination of parameters. We find $A = 22.2$ and $B = 1380$ K. At 340 K this corresponds to an apparent activation energy of 114 kJ/mol: it increases with decreasing temperature up to 425 kJ/mol at 280 K. These values are in the range of activation energies determined for LCP with the same mesogen [13].

The inset in the figure gives an overview of the relaxation behavior including the β process. The latter is observed in both frequency ranges of the experiment and its temperature variation may be described by a single Arrhenius law covering the full range: $\ln \tau^{-1} = A - E_a/RT$. The activation energy is 35 kJ/mol. Within error the same value is also found for both GxM11. These differ,

however, with respect to the limiting frequency at high temperature, i.e. the parameter A. It is 32.7 for G1M5 but is larger for G1M11 (A = 34.1) and G2M11 (A = 34.7). The activation energy is significantly larger than that found for the same dendrimers with -C_6F_{13} end groups. The β process is therefore strongly dependent on the nature of the end group. As opposed to LCPs the β process in the dendrimers varies with the length of the spacer. No variation was observed in LCPs with spacer lengths varying from 2 to 11 [16]. Various microscopic mechanisms may give rise to a fast relaxation in the dielectric spectroscopy of LCPs. They may be related to motions of the spacer or of the polymer backbone itself, as well as to the mesogen dynamics. From a comparison of the two series of dendrimers with very different end groups we believe its microscopic origin to be a rotational relaxation of the end group around its long axis. This is a local process which is influenced by spacer length only indirectly through the packing density.

As previously mentioned both dendrimers with long spacers possess a low-temperature phase of high order within the smectic layers before transforming into the glassy state at very low temperature. Fortunately the transition between the S_E and the S_A phase occurs at temperatures that are easily accessible in the dielectric spectroscopy experiment. We are therefore able to follow the δ process through the phase transition. The change in order has a strong impact on the relaxation time of the δ process as well as on the relaxation strength. This is shown for G2M11 in Fig. 6.

Three spectra are displayed that refer to temperatures in the immediate vicinity of the phase transition in the S_E and in the S_A phases. The phase transition is seen in a jump in the relaxation time, τ, and in an abrupt change in the relaxation strength. We also observe a stronger d.c. contribution to the dielectric loss in the S_A phase. No change is seen in the line shape of the relaxation, however. The transition temperature as determined from this measurement during cooling is significantly lower than that given in Table 1 based on the DSC results in a heating run. The origin for this apparent discrepancy lies in the heating rate of the DSC measurement. The additional order that is introduced into the smectic layers at the phase transition increases the relaxation time of the δ process.

The full temperature variation of the δ process for the three dendrimers is depicted in Fig. 7. Fig. 7b shows the variation of the relaxation strength, $\Delta\varepsilon$. In the case of G1M5 we find a continuous decrease nearly proportional to the reciprocal temperature as would be expected from the Onsager equation for rigid rotating dipols. Both dendrimers with long spacers, however, exhibit a stepwise increase in $\Delta\varepsilon$ at their respective phase transition from S_E to S_A. The step height is 2 for G2M11 but 3 in the case of G1M11. The effective dipole moment that becomes active to contribute to the δ relaxation at the transition temperature is much larger for G1M11.

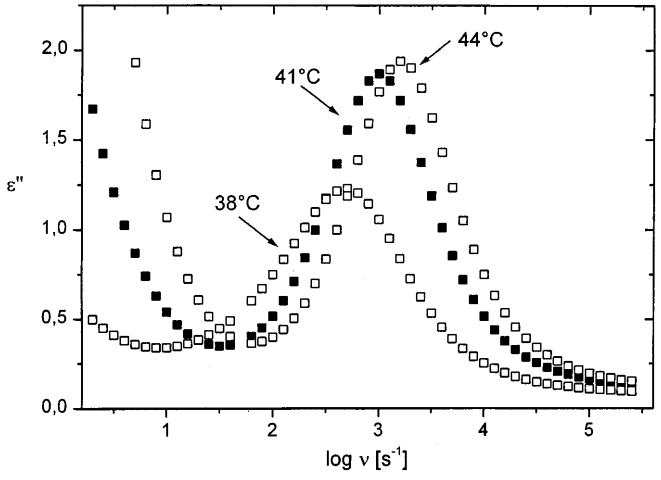

Fig. 6 The transition from S_E to S_A is clearly seen in ε'' for G2M11. Three temperatures in the vicinity of the phase transition are shown

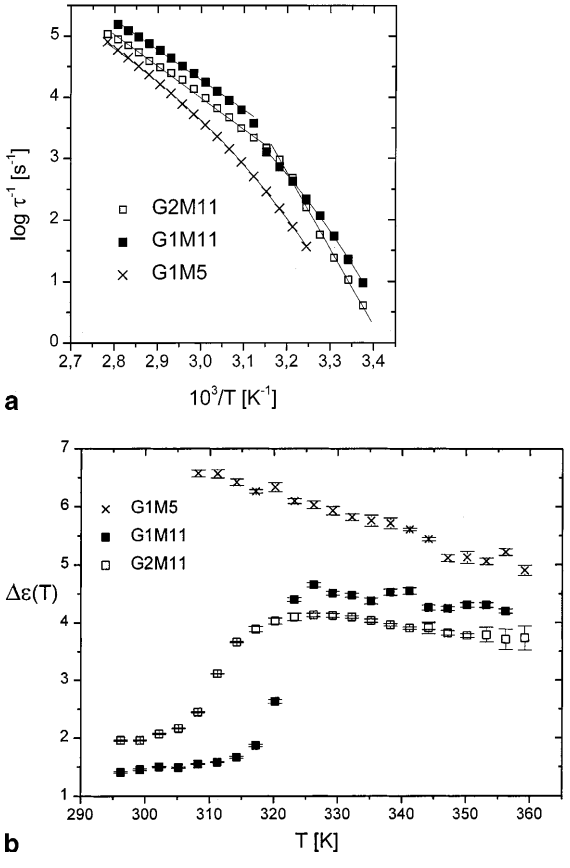

Fig. 7a, b Comparison of the temperature dependence of the δ process for the three dendrimers. The impact of the transition from S_E to S_A is obvious for the dendrimers with long spacers. In **a** the relaxation time, τ, is shown, while **b** displays the relaxation strength

Above the phase transition, $\Delta\varepsilon$ again begins to decrease according to the same law that is found for G1M5. The variation of the relaxation time with temperature is given in Fig. 7a in an Arrhenius diagram. In the S_A phase both dendrimers G1M11 and G2M11 show a linear dependence of log τ with reciprocal temperature. The temperature variation is governed by the activation energy of 95($\pm$2) kJ/mol. G1M5 apparently attains the same value at high temperature as is suggested by the nearly parallel curves in Fig. 7. A striking difference between G1M11 and G2M11 is the absolute value of the relaxation time. Although the spacer length is the same G1M11 displays a faster relaxation. This may be related to the lateral packing density in the smectic layers (see earlier) which is higher for G2M11. The effect of the dendrimer core in this respect differs from that of a simple spacer. The arrangement of the mesogens on the surface of the dendrimer scaffold couples the lateral order of the mesogens to the deformation of the dendrimer. The second generation dendrimer is more flexible and is such able to accommodate a better packing of the mesogens.

Just below the transition into the S_E phase the relaxation time for both dendrimers is the same. The lateral order within the smectic layers has changed but the same conditions are now provided for the δ relaxation. The temperature dependence in this phase differs greatly from that in the S_A phase. The apparent activation energy is larger. For G2M11 it is increased by a factor 2.5, but for G1M11 this factor is only 1.9. Close inspection of the data in Fig. 7 shows, however, that the relaxation time for G1M11 does not follow a simple Arrhenius law. The curve is clearly bent, indicating a coupling of the observed δ relaxation to the relaxation modes of the dendrimer backbone. This coupling is stronger in the case of the short spacer leading to the Vogel–Fulcher-type temperature dependence found for G1M5 in the full temperature range. G2M11 is more flexible as is expressed in its lower T_g (Table 2) and the coupling is therefore less effective.

Conclusion

The overall features of the dielectric relaxation in dendrimers with liquid-crystalline end groups resemble the behavior of conventional LCPs; however, two differences should be pointed out. The β process in the dendrimers varies with spacer length as opposed to the findings for LCPs. The dependence of the local mobility of the end groups may, therefore, not be traced back to the decoupling effect of the spacer alone. It is the ellipsoidal shape of the dendrimer scaffold that deviates strongly from the planar form preferred by the end groups and that consequently gives rise to a deformation of local order in between the mesogens. Increasing spacer length relaxes this constraint and allows the mesogens to rearrange. The second observation refers to the narrow width of the δ process. This is taken as an indication for a clear separation between the relaxation times of the dendrimer scaffold and the end groups. The distortion of the dendrimer scaffold as a consequence of the smectic order within the end groups may be responsible for a shift in its relaxation times. The interplay between the planar arrangement of the mesogens and the basically spherical architecture of the dendrimer scaffold strongly influences the relaxation behavior of the end groups.

The impact of order on the relaxation time is clearly observed at the transition from the S_E to the S_A phase. It leads to a discontinuous decrease in the relaxation time.

Acknowledgements Financial support of this work by the BMBF (grant no. 03-ST5-FRU-8) is gratefully acknowledged.

References

1. Collyer AA (ed) (1992) Liquid crystal polymers: from structures to applications. Elsevier, Amsterdam
2. (a) Chen SH, Mastrangelo JC, Shi H, Bashir-Hashemi A, Li I, Gelber N (1995) Macromolecules 28:7775; (b) Chen SH, Mastrangelo JC, Shi H, Blanton TN, Bashir-Hashemi A (1997) Macromolecules 30:93; (c) Hölter D, Frey H, Mülhaupt R, Klee JE (1996) Macromolecules 29:7003
3. Lorenz K, Hölter D, Stühn B, Heck B, Mülhaupt R, Frey H (1998) Chem Eur J (Submitted)
4. Lorenz K, Frey H, Stühn B, Mülhaupt R (1997) Macromolecules 30:6860
5. Stark B, Stühn B, Frey H, Lach C, Lorenz K, Frick B (1998) Macromolecules 31:5415
6. Trahasch B, Stühn B, Frey H, Lorenz K (1999) Macromolecules 32:1962
7. Zentel R, Strobl GR, Ringsdorf H (1985) Macromolecules 18:960
8. Stühn B, Stickel F (1992) Macromolecules 25:5306
9. Lorenz K, Mülhaupt R, Frey H, Rapp U, Mayer-Posner FJ (1995) Macromolecules 28:6657
10. (a) Sukruk V, Wendorff JH, Percec V, Lee M (1993) Polymer 34:481; (b) Duran R, Guillon D, Gramain P, Skoulios A (1987) Makromol Chem Rapid Commun 8:181
11. (a) Klinbiel RT, Genova DJ, Crisswell TR, Van Meter JP (1974) J Am Chem Soc 96:7651; (b) Hedvig P (1977) Dielectric spectroscopy of polymers. Hilger, Bristol
12. (a) Havriliak S, Negami S (1966) J Polym Sci Part C 14:99; (b) Havriliak S, Negami S (1967) Polymer 8:161
13. Zhong ZZ, Schuele DE, Gordon WL (1994) Liq Cryst 17:199
14. Martin A, Meier G, Saupe A (1971) Symp Faraday Soc 5:119
15. Davies M, Moutran R, Price AH, Beevers MS, Williams G (1976) J Chem Soc Faraday Trans II 72:1447
16. Schdrnfeld A, Kremer F, Hofmann A, Kuhnpast K, Springer J, Scherowsky G (1993) Makromol Chem 194:1149